Elastic Scattering of Protons by N^{14}†

F. B. HAGEDORN, F. S. MOZER, T. S. WEBB, W. A. FOWLER, AND C. C. LAURITSEN
Kellogg Radiation Laboratory, California Institute of Technology, Pasadena, California
(Received September 28, 1956)

The cross section for the elastic scattering of protons by N^{14} has been measured at center-of-mass angles of 90°, 125°, 154°, and 160° for proton energies between 620 and 1820 kev. Anomalies were observed at 1054±3, 1544±6, 1737±4, and 1799±5 kev. If one assumes that the nonresonant cross section results from only *s*-wave potential scattering, the assignments $J=3/2^+$ at 1054 kev and $J=1/2^+$ at 1544 kev are deduced. Fitting of the 1737-kev anomaly has not been found possible if one assumes a pure *s*-wave background. This uncertainty in background also prevents a definitive analysis of the 1799-kev data. However, qualitative theoretical fits of the 1799-kev data are obtained for *p*-wave formation of either a $J=1/2^-$ or $3/2^-$ state.

I. INTRODUCTION

THE study of the elastic scattering of protons by N^{14} is of interest in connection with the information which may be obtained regarding excited states of the compound nucleus O^{15}. Several levels in O^{15} in the present energy range have previously been reported by Duncan and Perry[1] from the study of $N^{14}(p,\gamma)$, and investigations of the elastic scattering at proton energies above 1 Mev have recently been reported by Tautfest *et al.*,[2] Gove *et al.*,[3] and Ferguson *et al.*[4] A preliminary report of the present results has previously been given.[5]

II. EXPERIMENTAL PROCEDURE

Protons were accelerated by the 2-Mev electrostatic accelerator at this laboratory and were analyzed by an 80-degree electrostatic analyzer which maintained the beam homogeneous in energy to better than 0.1%. The proton beam was scattered from targets placed at the object position of a 180-degree double-focussing magnetic spectrometer which is so mounted as to allow a continuously variable scattering angle from 0 to 160 degrees with respect to the incident beam direction. The scattered protons were detected by a cesium iodide scintillation counter placed near the exit slit of the magnetic spectrometer. The calibration of the apparatus has previously been described in detail.[6]

Thin-target yields were obtained from the thick targets by observing a given interval of the momentum spectrum of the scattered protons using the magnetic spectrometer. This technique has been previously discussed by Brown *et al.*[7] and Snyder *et al.*[8] who give the appropriate expressions for obtaining the cross section and reaction energy. It should be noted that this technique is practical only for solid target material which contains no extraneous nuclei heavier than those from which the scattering is to be observed.

The preparation of such nitrogen targets presented a considerable problem. Attempts were made to use ammonia (NH_3), lithium nitride (Li_3N), beryllium nitride (Be_3N_2), and adenine ($C_5N_5H_5$). Of these, Li_3N is extremely unstable to decomposition under the action of water and proved to be of no value as a target material. Solid ammonia targets, frozen on liquid nitrogen cooled rods, failed because of target contamination and deterioration under bombardment. Since the yields from various beryllium nitride targets differed by as much as 20%, the composition of such targets was uncertain, making them unsuitable for measuring absolute cross sections. Evaporated adenine targets produced yields reproducible to within 3% and withstood prolonged bombardment by one microampere beams. For this reason the absolute normalization of all the cross section data was done with this type of target.

In addition to these thick targets, considerable use has been made of thin targets prepared by the bombardment of a clean beryllium surface with a nitrogen ion beam of several kilovolts energy.[9] By using 10-kev nitrogen ions a target 1 kev thick to 1.7-Mev protons was produced and was used in the investigation of the regions near 1.05 Mev and 1.7 Mev to 1.8 Mev. Twenty-

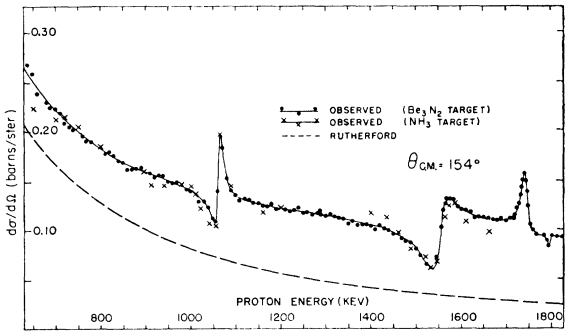

FIG. 1. The elastic scattering of protons by N^{14} at $\theta_{c.m.}=154°$.

† Supported in part by the joint program of the Office of Naval Research, and the U. S. Atomic Energy Commission.

[1] D. B. Duncan and J. E. Perry, Phys. Rev. **82**, 809 (1951).
[2] Tautfest, Havill, and Rubin, Phys. Rev. **98**, 280(A) (1955); and G. W. Tautfest and S. Rubin, Phys. Rev. **103**, 196 (1956).
[3] Gove, Ferguson, and Sample, Phys. Rev. **93**, 928(A) (1954).
[4] Ferguson, Clark, Gove, and Sample, Chalk River Project Report PD-261, 1956 (unpublished).
[5] Webb, Li, and Fowler, Phys. Rev. **92**, 1084(A) (1953).
[6] Webb, Hagedorn, Fowler, and Lauritsen, Phys. Rev. **99**, 138 (1955).
[7] Brown, Snyder, Fowler, and Lauritsen, Phys. Rev. **82**, 159 (1951).
[8] Snyder, Rubin, Fowler, and Lauritsen, Rev. Sci. Instr. **21**, 852 (1950).
[9] F. B. Hagedorn, Phys. Rev. **100**, 1793(A) (1955).

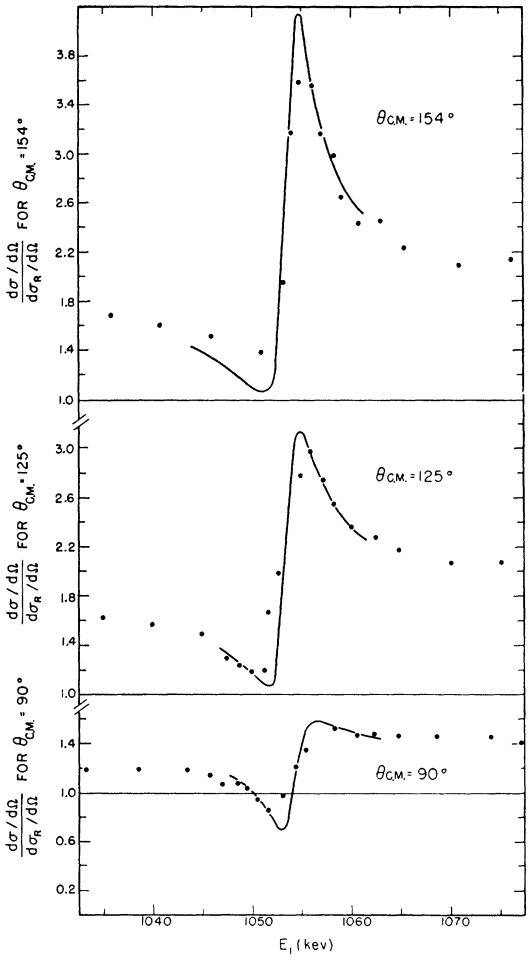

FIG. 2. The 1054-kev resonance in $N^{14}(p,p)$. The solid curve is the theoretical fit for s-wave formation of a 3-kev wide $J=3/2^+$ state.

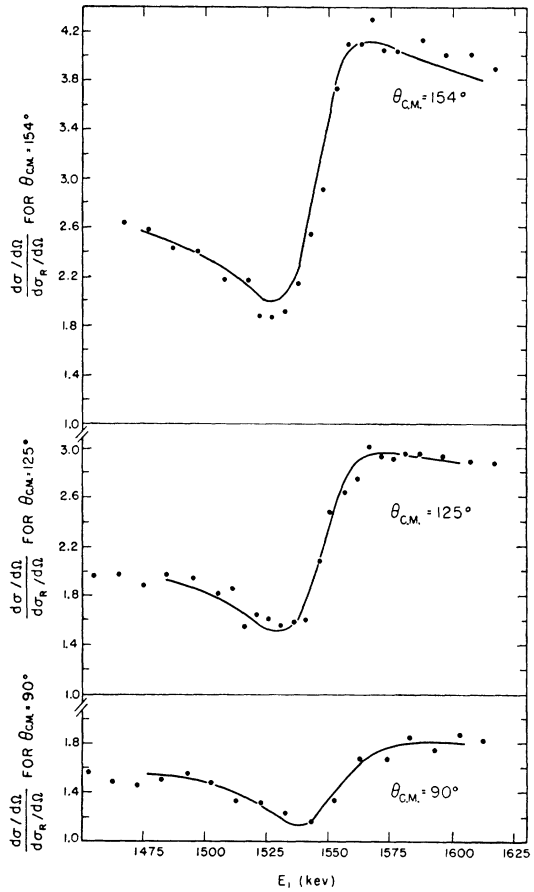

FIG. 3. The 1544-kev resonance in $N^{14}(p,p)$. The solid curve is the theoretical fit for s-wave formation of a 34-kev wide $J=1/2^+$ state.

kev nitrogen ions produced targets 2 kev thick to 1.7-Mev protons and were used for the other thin target measurements.

The primary disadvantage in the use of thin targets prepared in this way is the fact that the nitrogen content is not precisely known and absolute cross section values cannot be determined. The relative thin-target cross sections, normalized to the thick-target data of Fig. 1, were obtained from the peak yield of the momentum profile in the manner discussed by Brown *et al.*[7]

To obtain the absolute scattering cross section from the thick-target yield, the stopping cross section for protons per N^{14} nucleus in adenine was needed. This quantity was calculated by adding the stopping cross sections of carbon, nitrogen, and hydrogen. The carbon and nitrogen stopping cross sections were obtained from the stopping cross section formula,[10] with the K-shell correction term C_K calculated from the values given by Walske.[11]

Mather and Segrè[12] have measured the carbon ionization potential to be 74.4 volts, and the values for the stopping cross section computed using this ionization potential agree well with the carbon stopping cross sections below 600 kev given by Reynolds, Dunbar, Wenzel, and Whaling,[13] which are average values obtained by subtracting the hydrogen contribution from the measured stopping cross sections of several hydrocarbons. The nitrogen stopping cross section has been measured below 1.0 Mev by Chilton, Cooper, and Harris[14] and below 600 kev by Reynolds *et al.* In the region of overlap, these measurements are in good agreement, and from them, an ionization potential of 90 volts was deduced. By applying the appropriate conversions, the stopping cross section for protons in hydrogen was obtained from the stopping cross section for alpha

[10] H. A. Bethe and J. Ashkin, *Experimental Nuclear Physics*, edited by E. Segrè (John Wiley and Sons, Inc., New York, 1953), Vol. I, Part II.

[11] M. C. Walske, Phys. Rev. **88**, 1283 (1952).

[12] R. Mather and E. Segrè, Phys. Rev. **84**, 191 (1951).

[13] Reynolds, Dunbar, Wenzel, and Whaling, Phys. Rev. **92**, 742 (1953).

[14] Chilton, Cooper, and Harris, Phys. Rev. **93**, 413 (1954).

particles in hydrogen as measured by Mano.[15] Reynolds *et al.* have measured the stopping cross section in hydrogen for protons of energies less than 600 kev, and the values given by Mano are in excellent agreement from 500 to 600 kev after the appropriate conversion has been made.

The final normalization of the cross section was done at an incident proton energy of 1149 kev. The stopping cross section per N^{14} nucleus for protons in adenine was required at incident and scattered proton energies of 1149 and 875 kev, respectively. The values used were 9.89×10^{-15} ev-cm^2 and 11.87×10^{-15} ev-cm^2.

III. EXPERIMENTAL RESULTS

The results of these investigations are presented in Fig. 1 as the observed cross section for proton energies from 0.62 to 1.82 Mev at a center-of-mass scattering angle of 154°, and in Figs. 2 through 5 as the ratio of the observed cross section to the Rutherford cross section at angles of 90°, 125° and 154° or 160°, at energies near the 1054, 1544, 1737, and 1799-kev resonances.

The cross section for the elastic scattering of protons by N^{14} has been obtained from the calibrations of the magnet acceptance solid angle and resolution, counter efficiency, and current integrator firing charge, as determined by the assumed Rutherford scattering of protons in copper. The ratio of the yield of elastically scattered protons from the nitrogen in a thick adenine target to that from copper in a freshly evaporated copper target at a scattering energy of 1149 kev and center-of-mass scattering angle of 154° resulted in a value of 128 millibarns/steradian for the nitrogen cross section. The 4% uncertainty in the stopping cross section of protons in copper thus contributes to the total uncertainty in the nitrogen absolute cross section determination. Considering the stopping cross sections of protons in carbon, nitrogen, and hydrogen known to within 4%, the stopping cross section per N^{14} nucleus for protons in adenine is uncertain by about 6%. Sufficiently large numbers of counts were taken to make statistical uncertainties negligible, as was the 0.3% uncertainty in the firing voltage of the current integrator. The uncertainties in stopping cross sections, when compounded with the probable errors in the energy and angle measurements and with the variations of the different adenine targets, result in a total uncertainty of 8% in the elastic scattering cross section given above.

Measurement of the carbon yield from the thick adenine targets resulted in independent verifications of two assumptions implicit in the determination of the absolute nitrogen cross section. Since the ratio of the carbon to nitrogen elastically scattered proton yields remained constant both under bombardment and from one target to another, the possibility of the deterioration of the adenine during evaporation or bombardment has been eliminated, thereby justifying the use of $C_5N_5H_5$ as the chemical composition of the target material. In addition, the elastic scattering cross section for protons by carbon has been calculated from the carbon yield. The result of this calculation is 198 millibarns/steradian at a center-of-mass scattering angle of 154.2° and a scattering energy of 1149 kev. This is to be compared with 203 millibarns/steradian[16] reported by Jackson *et al.*[17] This agreement demonstrates the validity of the

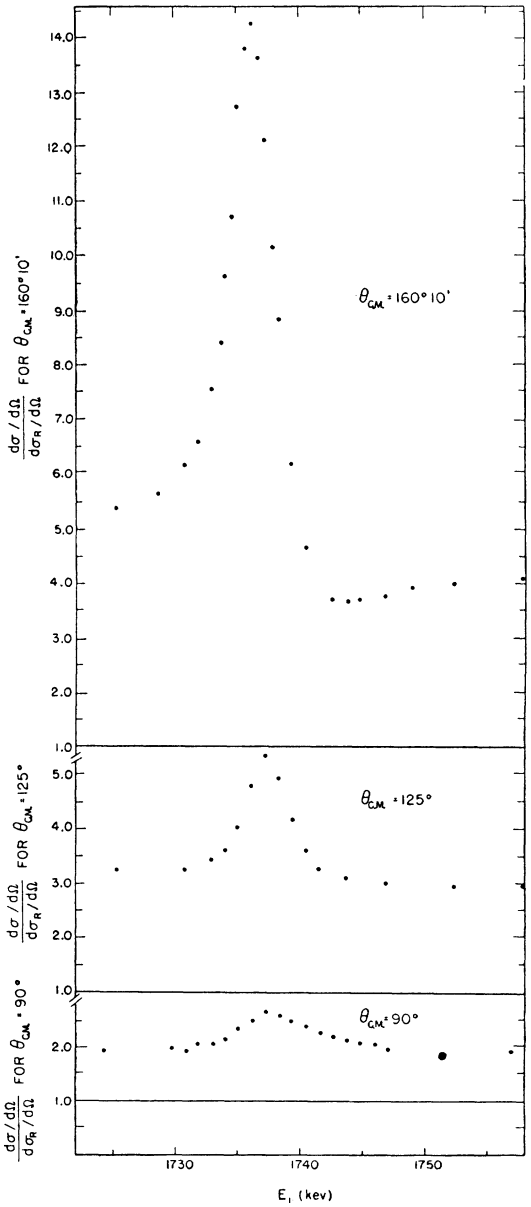

FIG. 4. The 1737-kev resonance in $N^{14}(p,p)$.

[15] G. Mano, Ann. Phys. 1, 407 (1934).

[16] This value was obtained by interpolating in angle from the published graphs and is uncertain by about 6%.

[17] Jackson, Galonsky, Eppling, Hill, Goldberg, and Cameron, Phys. Rev. 89, 365 (1953).

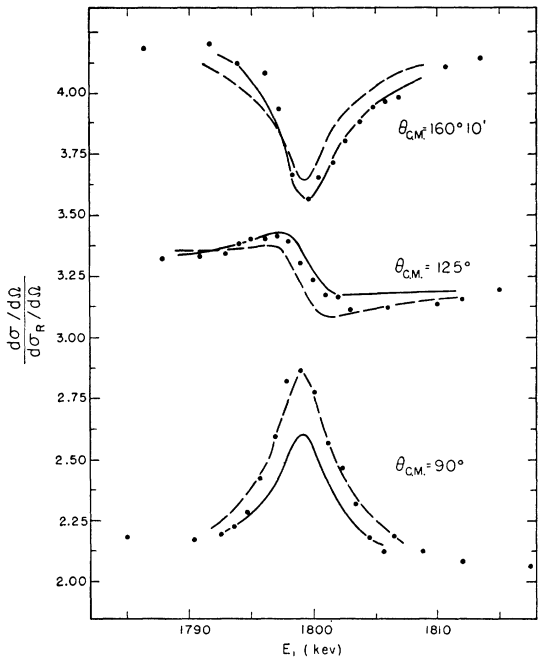

FIG. 5. The 1799-kev resonance in $N^{14}(p,p)$. The solid and dashed curves are respectively the fits for p-wave formation of 4-kev wide $J=1/2^-$ and $J=3/2^-$ states.

assumptions made in order to establish the stopping cross section for protons in adenine.

For other energies at a center-of-mass scattering angle of 154°, the cross sections were measured relative to the one chosen for normalization to an accuracy of about 1% using thick targets. Using thin targets, the cross sections at 125° and 90° were measured relative to that at 154° to an accuracy of about 6% and 11%, respectively.

The absolute value of the cross section is of considerable importance in analyzing scattering data, so it is significant to compare this quantity as determined by the present experiment with other measurements. Table I presents this comparison at three energy regions in which the nonresonant cross section is changing relatively slowly.

Reasonable agreement is seen to exist between the present experiment and the data of Ferguson *et al.*,[4] while the data of Tautfest and Rubin[2] appears consistently low. Earlier measurements made in this laboratory were in better agreement with Tautfest and Rubin, but this was a result of normalizing with the NH_3 and Be_3N_2 targets. It is currently believed that the chemical composition of these targets was different from that assumed, resulting in the use of incorrect stopping cross sections. As pointed out above, data from neither Be_3N_2 nor NH_3 were reproducible, implying that there were significant chemical variations.

In addition to differences in the absolute normalization, the data reported herein differ from those of the other observers in the size of the anomalies reported at 1054, 1737, and 1799 kev. Unfortunately, this difference is possibly a compounding of two effects. The first of these two is that changing the absolute normalization changes the measured anomaly size proportionately.

The second effect is the decrease in anomaly size caused by finite energy resolution. The magnitude of this effect has been calculated in reference 6 for a square energy-resolution window. It is of interest for the consideration of narrow resonances to plot the decrease of experimental anomaly size that results from this effect. In this plot the same notation as in reference 6 will be used except for the substitution of Eq. (1) of this paper, given below, for Eq. (B1) of the above reference. These two equations are equivalent expressions of the differential scattering cross section uncorrected for effects of finite resolution. This change of equation requires that the $c=a/b$ of reference 6 be replaced by $c=|S/A|$. Figure 6, which is a graph of Eq. (B7) of reference 6, demonstrates the variation of k with α for various values of $|S/A|$, where k is the fractional decrease in anomaly size resulting from finite energy resolution and $\alpha\Gamma$ is the full energy resolution window width, Γ being the true width of the resonance in question.

It is clear from Fig. 6 that substantial decreases in anomaly size may result from finite energy resolution. One must therefore be exceedingly careful in using the experimentally measured size of an anomaly in making an analysis of elastic scattering data if the resonance is not definitely known to have a width of at least a few times the window width. During the present experiment, the window width, estimated from the thickness of the targets and from the energy spread of the incident proton beam, was between one and two kev in the energy region between 1.0 and 1.8 Mev.

The experimental results are tabulated in Table II which also lists the various parameters of the excited states of O^{15} as determined by the following analysis. E_R is the resonance energy in Mev in the laboratory system for the incident protons on an N^{14} target nucleus. $E(O^{15*})$ is the excitation energy in Mev of the corresponding excited state in O^{15} and Γ is the observed resonance width in kev in the laboratory coordinate

TABLE I. Comparison of absolute cross sections.

E_p (kev)	θ (cm)	$d\sigma/d\Omega$ (mb/sterad)	Observer
900	152°	138	Tautfest and Rubin[a,b]
900	154°	155±12	Present experiment
1316	152°	100	Tautfest and Rubin
1316	155.2°	121.6±5.7	Ferguson *et al.*[c]
1316	154°	119±9	Present experiment
1679	152°	104	Tautfest and Rubin
1679	155.2°	113.3±3.7	Ferguson *et al.*
1679	154°	112±9	Present experiment

[a] The data from Tautfest and Rubin have been taken from the published graphs, making the third digit questionable.
[b] See reference 2.
[c] See reference 4.

system. The tabulated results indicate some differences in E_R and Γ from those of Duncan and Perry[1] as obtained from $N^{14}(p,\gamma)$. Their energy scale would seem to be approximately 1% too high and the larger values for the widths seem to suggest somewhat poorer energy resolution in their experiments.

In the last columns of Table II, θ^2 indicates the fraction of the single particle limit for the width of each level as calculated from the measured width and the curves of Christy and Latter.[18] The letters in parentheses indicate the l value for which θ^2 is calculated. The quantity $\omega\Gamma_\gamma$ is the product of the statistical factor and radiation width, and is determined from the data of Duncan and Perry[1] corrected to the resonance widths determined in this experiment. The product is divided into the two separate factors in the cases where the assignment has been suggested by this experiment. Also given are the l values for the proton capture by N^{14} and the spin and parity (J,π) for each state where determined.

IV. ANALYSIS OF THE EXPERIMENTAL RESULTS

In the region of isolated single resonances the theoretical ratio of the differential elastic scattering cross section to the Rutherford cross section may be expressed as:

$$\frac{d\sigma/d\Omega}{d\sigma_R/d\Omega}=B(E,\theta)+A(E,\theta)\sin\delta\cos\delta+S(E,\theta)\sin^2\delta, \quad (1)$$

where the resonant phase shift δ is given by

$$\cot\delta=\frac{E_R-E}{\Gamma/2},$$

and

$$d\sigma_R/d\Omega=(0.06350/E^2)\csc^4(\theta/2)\ \text{barns/steradian},$$

where E and θ are, respectively, the incident proton energy in Mev and the scattering angle, both measured in the center-of-mass system.

In the narrow level approximation of elastic scattering analysis, the energy variations of the nonresonant scattering amplitude, de Broglie wavelength, and Rutherford scattering amplitude are assumed to be negligible over the region of the narrow resonance. Thus the energy dependences in the background term $B(E,\theta)$ and the coefficients $A(E,\theta)$ and $S(E,\theta)$ are removed.

TABLE II. Parameters of excited states of O^{15}.

E_R Mev	$E(O^{15*})$ Mev	Γ kev	θ^2	$\omega\Gamma_\gamma$ ev	l	J,π
1.054 ±0.003	8.33	3±1	0.0029 (s)	$\frac{2}{3}\times0.59$	0	$3/2^+$
1.544 ±0.006	8.79	34±4	0.016 (s)	$\frac{1}{3}\times0.33$	0	$1/2^+$
1.737 ±0.004	8.97	4±1	0.0013 (s) 0.017 (d)	0.076	···	$\leq 5/2^a$
1.799 ±0.005	9.03	4±1	0.0028 (p)	$\frac{2}{3}\times0.45$ $\frac{1}{3}\times0.90$	1	$3/2^-$ $1/2^-$

[a] Determined from the observed gamma-ray width.

[18] R. F. Christy and R. Latter, Revs. Modern Phys. **20**, 185 (1948).

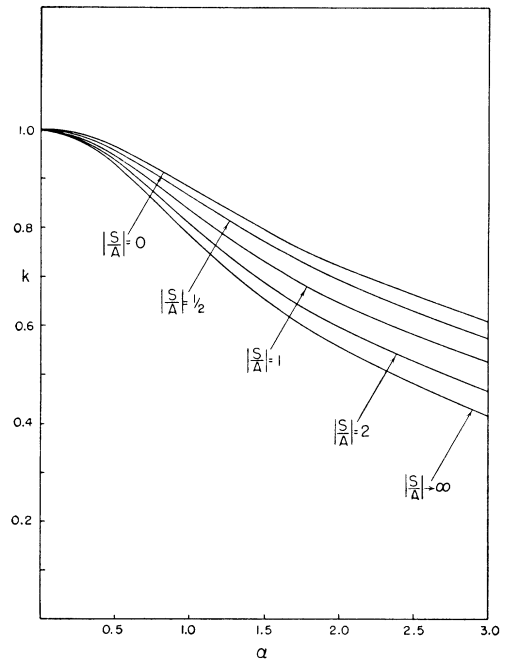

FIG. 6. The decrease of the anomaly size due to finite resolution effects, where k is the fractional decrease in anomaly size resulting from finite resolution, and α is the ratio of the energy resolution width to true resonance width.

As a first step in the analysis of such isolated narrow resonances, curves of the ratio of experimental to Rutherford cross sections *versus* energy are fitted to Eq. (1), assuming $B(\theta)$, $A(\theta)$, $S(\theta)$, E_R, and Γ to be arbitrary parameters, values of which are determined by the best agreement between the above equation and the experiment. The second step is then to compare the angular variations of these experimentally determined parameters with those obtained from theory for various choices of the spin and parity of the resonant state and the nature of the background, in an attempt to deduce the properties of the resonant state. Since this fitting of n excitation curves with an equation similar to (1) requires the determination of $3n+2$ unknowns, none of the unknowns can be determined with a high degree of accuracy. It is for this reason that the widths of the narrow resonant states listed in Table II contain uncertainties of as much as 20%, independent of the previously discussed resolution effects that also contribute to an uncertainty in observed width.

Throughout the following discussion of the analysis of the N^{14} elastic scattering data, it is assumed, unless otherwise specifically noted, that the deviation of the nonresonant scattering from the Rutherford cross section arises only from s-wave potential scattering. This

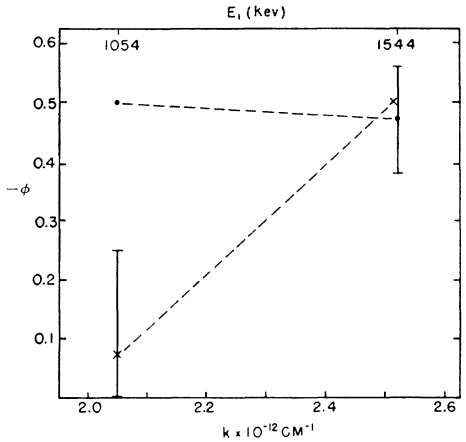

FIG. 7. The s-wave potential phase shifts as determined from their interference effects and contributions to the background at the various resonances. The dots and crosses represent the $J=1/2$ and $J=3/2$ s-wave potential phase shifts, respectively.

assumption introduces the two unknown s-wave potential phase shifts $\phi_{1/2}$ and $\phi_{3/2}$, where the subscripts refer to the channel spin in which the potential scattering occurs. The s-wave potential phase shifts are determined both from their interference with the resonance amplitudes and from the nonresonance angular distributions. The details of these determinations will be given in the following discussion of the states of O^{15} which were investigated in the present experiment.

The anomaly near 1054-kev proton bombarding energy exhibits interference minima at both 90° and 125°, a behavior consistent only with at least partial s-wave formation,[19] since higher than f-waves are ruled out by the Wigner criterion. The predicted anomaly for s-wave formation of a $J=3/2$ state with the interfering s-wave potential phase shift $\phi_{3/2}$ equal to -0.08 radian, illustrated in Fig. 2, is seen to be in reasonable agreement with experiment. The $J=1/2$ s-wave anomaly size, being half that for $J=3/2$, is too small.

A plot of $-\phi_{1/2}$ and $-\phi_{3/2}$ *versus* the wave number k is given in Fig. 7. In this figure the points containing estimates of errors are deduced from the interference between the s-wave potential scattering amplitude and the resonant amplitude. The points without estimates of errors result from fitting the nonresonant angular distributions with one unknown s-wave potential phase shift, considering the other potential phase shift obtained from the resonance interference as known. In this manner $\phi_{1/2}$ at 1054 kev was determined to be -0.50 radian.

The 1544-kev resonance, also displays interference anomalies at all angles of observation and must therefore be at least partially formed by s-wave protons. Since the theoretical anomaly size for $J=3/2^+$ is twice as large as that illustrated in Fig. 3 for $J=1/2^+$, it is concluded that the 1544-kev resonance is s-wave $J=1/2^+$. The interfering s-wave potential phase shift $\phi_{1/2}$ is deduced from the resonance analysis to be -0.47 radian. The value for $\phi_{3/2}$ is then determined from this value of $\phi_{1/2}$ and the nonresonant angular distribution to be -0.50 radian. The theoretical anomaly size being given exactly for the case of an s-wave resonance interfering with an s-wave background, the agreement between experiment and theory at 1544 kev might be taken as confirmation of the absolute normalization. However, the interference between the non s-wave part of the background and the s-wave resonant state may possibly be large enough to negate this conclusion.

The 1799-kev resonance anomaly, being positive and symmetric about the resonance energy only at 90° is therefore likely formed by odd orbital angular momentum protons, since only for such cases do all interference effects disappear at 90° unless a cancellation of interfering terms happens, by chance, to occur. If one assumes p-wave formation of the compound state, the 90° anomaly size is determined if its spin is 1/2 or 5/2, while for $J=3/2$ the anomaly is dependent upon a channel spin ratio. Since the calculated $J=5/2$ anomaly is about twice that experimentally observed, this choice of spin for the compound state is ruled out. The theoretical excitation curves illustrated in Fig. 5 are obtained for $J=1/2$, $\phi_{3/2}=-0.32$ radian and channel spin amplitude $\alpha_{3/2}=1$ ($\phi_{1/2}$ is undetermined because $\alpha_{1/2}=0$); and for $J=3/2$, $\phi_{3/2}=-0.32$ radian, $\phi_{1/2}=-0.45$ radian, and $\alpha_{3/2}{}^2=0.17$. It should be pointed out that these values of channel spin amplitudes and potential phase shifts may be varied over rather large limits without altering the general character of the theoretical excitation curves, hence no plot of these s-wave potential phase shifts is included in Fig. 7.

Since both $J=1/2$ and $J=3/2$ are at least in qualitative agreement with experiment, and since the inclusion of the non s-wave amplitudes in the background that will be required to explain the 1737-kev anomaly will also affect the 1799-kev resonance, it is impossible to decide from the present experiment between the two possible choices for the spin of the 1799-kev state. However the general agreement of either assignment with experiment argues strongly in favor of p-wave formation of the resonant level.

It has not been found possible to obtain a satisfactory analysis of the 1737-kev resonance excitation functions of Fig. 4 for any allowed pure orbital angular momentum formation of a compound state interfering with an arbitrary pure s-wave background. The best such analysis, assuming s-wave potential phase shifts consistent with those obtained at neighboring resonances, occurs for d-wave formation of a $J=3/2^+$ state through the $J=1/2$ channel. These assumptions are consistent with experiment at the back angles but cannot explain the 90° anomaly. This failure is at-

[19] R. F. Christy, Report on Amsterdam Conference, 1956, Physica (to be published).

tributable either to the fact that the compound nucleus is formed by an admixture of two or more orbital angular momenta, or that the background is not pure s-wave. To test the former hypothesis, an analysis was attempted for the assumptions of a $J=3/2^+$ state formed by an admixture of s-wave and d-wave protons interfering with a pure s-wave background. It has not been found possible to explain the anomaly with these assumptions for any combination of channel spin or d-wave to s-wave proton width ratios and any s-wave potential phase shifts consistent with those of Fig. 7. Since p-f admixtures or other s-d admixtures seem to be ruled out by the gross inability of the theoretical expressions representing pure s-wave, p-wave, d-wave or f-wave formation of states other than $J=3/2^+$ to fit the experimental data, it is concluded that this failure results from the fact that the background is not pure s wave. A similar conclusion is reported by the Chalk River group.[4]

That this conclusion is consistent with the analysis of the present data at 1054 and 1544 kev is seen by studying the energy variation of the s-wave potential phase shifts as given in Fig. 7. Through application of causality arguments in the absence of a Coulomb field, Wigner[20] has deduced the inequality,

$$d\phi/dk > -R, \tag{2}$$

where R is the radius of interaction and is given by $R=R_0(A_0^{1/3}+A_1^{1/3})$. The energy variation of the s-wave $J=3/2$ potential phase shift between 1054 and 1544 kev indicates a violation of this inequality by as much as a factor of two, and thus the background analysis at 1054, and 1544 kev produces a set of questionable s-wave potential phase shifts.

The possibility that the background in the region near 1700 kev contains a contribution from the previously reported broad s-wave state near 2600 kev[1] has been investigated by applying a pure s-wave analysis to the Chalk River[4] angular distributions between 1800 and 2900 kev in a manner similar to that reported in a previous article on analysis of broad elastic scattering anomalies.[21] The conclusion from this analysis is that the deviation of the elastic scattering cross section from the Rutherford value above 2 Mev is not consistent with pure s-wave resonant and/or potential scattering since the theoretical curves based on this assumption could not be made to fit the experimental data. Furthermore, the s-wave phase shifts deduced from the qualitative fitting of these data gave no indication of an s-wave resonance above 2 Mev.

Thus one is forced to conclude that above about 1-Mev proton bombarding energies, substantial amounts of $l>0$ potential and/or resonant scattering are present and that the broad anomaly near 2600 kev may not result from s-wave formation of the compound state.

[20] E. P. Wigner, Phys. Rev. **98**, 145 (1955).
[21] F. S. Mozer, Phys. Rev. **104**, 1386 (1956).

TABLE III. Low-lying excited states of O^{15} and N^{15}.

Configuration	J, π	T	Width in $N^{14}(1^+)+p$
Hole states			
$(1s_{1/2})^4(1p_{3/2})^8(1p_{1/2})^3=(1p_{1/2})^{-1}$	$1/2^-$	1/2	large p-wave
$(1s_{1/2})^4(1p_{3/2})^7(1p_{1/2})^4=(1p_{3/2})^{-1}$	$3/2^-$	1/2	small
$(1s_{1/2})^3(1p_{3/2})^8(1p_{1/2})^4=(1s_{1/2})^{-1}$	$1/2^+$	1/2	small
One-particle excitation[a]			
$(p_{1/2})^{-2}(1^+)(1d_{5/2})^1$	$3/2^+, 5/2^+, 7/2^+$	1/2	large d-wave
$(2s_{1/2})^1$	$1/2^+, 3/2^+$	1/2	large s-wave
$(1d_{3/2})^1$	$1/2^+, 3/2^+, 5/2^+$	1/2	large d-wave
$(p_{1/2})^{-2}(0^+)(1d_{5/2})^1$	$5/2^+$	1/2, 3/2	small
$(2s_{1/2})^1$	$1/2^+$	1/2, 3/2	small
$(1d_{3/2})^1$	$3/2^+$	1/2, 3/2	small
Four-particle excitation			
$(1s_{1/2})^4(1p_{3/2})^7(1d, 2s)^4$	$3/2^-$	1/2	small
$(1s_{1/2})^3(1p_{3/2})^8(1d, 2s)^4$	$1/2^+$	1/2	small

Total number of states

State	$1/2^-$	$3/2^-$	$1/2^+$	$3/2^+$	$5/2^+$	$7/2^+$	
Number	1	2	6	5	4	1	(19 in all)

[a] Excitation to $2s$ or $1d$ configurations only.

Until the question of the background analysis in this energy region is settled, the determination of the spins and parities of the narrow levels, the amplitudes of which interfere with this background, must remain somewhat in doubt. This understanding of the background scattering might be facilitated by more detailed measurements of angular distributions between resonances in the energy region above about one Mev.

The present results show no indication of the broad s-wave level reported at 700 kev by Duncan and Perry.[1] The smallest theoretical anomaly to be expected from such a state at a scattering angle of 154° is at least as large as the Rutherford cross section. No anomaly as large as 25% of this value was experimentally observed.

V. COMPARISON OF THE MASS 15 MIRROR STATES WITH SHELL MODEL THEORY

It is of some interest to compare the results of the present analysis of the states of O^{15} with shell model theory and also with the states of the mirror nucleus N^{15}. In Table III the low-lying states to be expected in O^{15} and N^{15} on the basis of the shell model with spin-orbit splitting are enumerated. The table is based on a slight extension of the pioneer work of Inglis[22] and follows strict j-j coupling only for convenience in enumerating the expected low-lying states. There will, of course, be considerable configuration interaction and the states will represent complicated mixtures of the various configurations. O^{15} and N^{15} represent one nucleon holes in the closed $1s$ and $1p$-shells at O^{16}. To the $(1p_{1/2})^{-1}$ and the $(1p_{3/2})^{-1}$ hole states discussed by Inglis the $(1s_{1/2})^{-1}$, $1/2^+$ state is added. This is in accordance with the expectation that an adequate nuclear model would take into account the raising of the $1s_{1/2}$-shell due to the fact that the nuclear radius exceeds the radius of interaction with low relative orbital angular momentum for the four $1s_{1/2}$ particles.

[22] D. R. Inglis, Revs. Modern Phys. **25**, 390 (1953).

The lowest one-particle excitation states will involve exciting one of the $1p_{1/2}$ nucleons to the $1d_{5/2}$ or $2s_{1/2}$ configurations as discussed by Inglis and also to the $1d_{3/2}$ configuration. The spin-orbit splitting ($\sim$3 Mev from O^{17} and F^{17}) in the d states leads one to expect the $1d_{3/2}$ excitations to be at somewhat higher energies than the $1d_{5/2}$ or, in another form of expression, to contribute preferentially to the relatively more highly excited states. The two unexcited $p_{1/2}$ nucleons can have parallel spins ($J=1^+$, $T=0$) as in the ground state of N^{14} or antiparallel spins as in the first excited state, $N^{14*}=2.31$ Mev ($J=0^+$, $T=1$). Following the suggestion of Christy and Fowler,[23] one expects the lowest multiple-particle excitations to involve four particles rather than two or three as indicated by the large binding energy of Ne^{20} compared to O^{18} or F^{19}. The symbols $(1d,2s)^4$ in Table III indicate the lowest 0^+-state obtainable in principle from the $1d$ and $2s$ configurations. Finally it is noted that only those states based on the ground state of N^{14}, namely $(1p_{1/2})^{-2}(1^+)$, will be expected to have large reduced proton widths in the $N^{14}(p,p)$ or $N^{14}(p,\gamma)$ processes. Comments on these widths are given in the last column of Table III.

The state at 1054-kev proton bombarding energy corresponds to an excitation of 8.33 Mev in O^{15}. This state may well be the analogue of the 8.57-Mev state in N^{15} for which Sharp, Sperduto, and Buechner[24] find $l=0$ and $l=2$ neutron capture in $N^{14}(d,p')N^{15*}$. Thus the N^{15} state is required to have $J=1/2$ or $3/2$. Since shell-model theory predicts the $1d_{5/2}$ interaction to predominate at lower energies, and since $J=1/2$ cannot be formed by this interaction, the most reasonable choice for the spin of the 8.57-Mev state of N^{15} is $3/2$. This agrees with the value of the spin of the hypothesized mirror level in O^{15} as deduced from the present experiment.

The 1544-kev resonance represents an excited state in O^{15} at 8.79 Mev. It probably corresponds to the state at 8.32 Mev in N^{15} for which Sharp *et al.* find only $l=0$ neutron capture in the $N^{14}(d,p')N^{15*}$ stripping reaction. Since the 8.79-Mev state in O^{15} has a reduced width of the order of one percent of the Wigner limit, a reasonable major configuration for it and the 8.32-Mev state of N^{15} is $(p_{1/2})^{-2}(0^+)(2s_{1/2})^1$.

A possible shell-model interpretation of the 1799-kev state (9.03 Mev in O^{15}) is obtained if the state is assumed to be a $3/2^-$ hole whose low excitation energy arises from the relatively large binding of two protons and two neutrons in the last subshell. The first $3/2^-$ level in O^{15} is probably the bound level at 6.14 Mev which is formed by p-wave protons in the $N^{14}(d,n)$ stripping reaction ($1/2^-$ and $5/2^-$ are other possibilities on this basis however). If the 6.14-Mev state is $3/2^-$, a reasonable configuration for this level is $(1s_{1/2})^4(1p_{3/2})^7(1p_{1/2})^4$. A rough calculation along the lines proposed by Christy and Fowler[23] indicates that the energy separation between the two supposed $3/2^-$ states is $(Ne^{20}-O^{16})-(O^{16}-C^{12})=2.40$ Mev, in reasonable agreement with the observed value of 2.88 Mev. It should also be noted that the 9.03-Mev level has the small binding energy of 1.2 Mev for $C^{11}+\alpha$, as might be expected.

For completeness, mention should be made of the 277-kev state in $N^{14}(p,p)$ recently shown to be an s wave $J=1/2^+$ state by R. E. Pixley of this laboratory. This state, at 7.61-Mev excitation in O^{15}, probably corresponds to the 7.31-Mev state in N^{15} which has been shown by Sharp *et al.* to result from s-wave neutron capture in the $N^{14}(d,p')N^{15*}$ stripping reaction. These two states may be thought to arise primarily from the configuration $(p_{1/2})^{-2}(1^+)(2s_{1/2})^1$ listed in Table III.

IV. ACKNOWLEDGMENTS

The authors would like to express their gratitude to the Chalk River group[4] for supplying a preprint of their experimental data, and to Professor R. F. Christy and Professor T. Lauritsen of this laboratory for their helpful discussions of various problems connected with this experiment.

[23] R. F. Christy and W. A. Fowler, Phys. Rev. **96**, 851(A) (1954).

[24] Sharp, Sperduto, and Buechner, Phys. Rev. **99**, 632(A) (1955); and Massachusetts Institute of Technology Progress Report (February 28, 1955) (unpublished), p. 43.